

---

# 000 001 002 003 004 005 006 007 008 009 010 011 012 013 014 015 016 017 018 019 020 021 022 023 024 025 026 027 028 029 030 031 032 033 034 035 036 037 038 039 040 041 042 043 044 045 046 047 048 049 050 051 052 053 MULTIDIFFNET: A MULTI-OBJECTIVE DIFFUSION FRAMEWORK FOR GENERALIZABLE BRAIN DECOD- ING

Anonymous authors

Paper under double-blind review

## ABSTRACT

Neural decoding from electroencephalography (EEG) remains fundamentally limited by poor generalization to unseen subjects, driven by high inter-subject variability and the lack of large-scale datasets to model it effectively. Existing methods often rely on synthetic subject generation or simplistic data augmentation, but these strategies fail to scale or generalize reliably. We introduce *MultiDiffNet*, a diffusion-based framework that bypasses generative augmentation entirely by learning a compact latent space optimized for multiple objectives. We decode directly from this space and achieve state-of-the-art generalization across various neural decoding tasks using subject and session disjoint evaluation. We also curate and release a unified benchmark suite spanning four EEG decoding tasks of increasing complexity (SSVEP, Motor Imagery, P300, and Imagined Speech) and an evaluation protocol that addresses inconsistent split practices in prior EEG research. Finally, we develop a statistical reporting framework tailored for low-trial EEG settings. Our work provides a reproducible and open-source foundation for subject-agnostic EEG decoding in real-world BCI systems.

## 1 INTRODUCTION

Electroencephalography (EEG) is a widely used modality in brain–computer interfaces (BCIs), supporting applications from assistive communication to cognitive monitoring. Deep learning has improved decoding across motor imagery, SSVEP, and speech tasks Gu et al. (2025); Ahmadi & Mesin (2025); Lee & Lee (2022), yet generalizing to unseen subjects remains challenging due to high inter-subject variability and limited data Huang et al. (2023); Barmpas et al. (2023).

Subject-specific models require extensive per-user calibration Hartmann et al. (2018); Luo & Cai (2024), while multi-subject models struggle to generalize Rommel et al. (2022); Liu et al. (2022); Wu (2016). The alternative is to use two-stage pipelines that generate EEG via GANs or diffusion and then train decoders (Hartmann et al., 2018; Torma & Szegletes, 2025), but they suffer from low realism, artifact transfer, and inefficiencies.

We propose *MultiDiffNet*, a unified multi-objective diffusion framework that learns a shared latent space, eliminating the need for synthetic augmentation and enhancing generalization. To benchmark progress, we release a curated suite spanning SSVEP, Motor Imagery, P300, and Imagined Speech tasks, with standardized subject- and session-disjoint evaluation. We also develop a statistical reporting protocol tailored for low-trial EEG research, addressing a persistent gap in reproducibility.

## 2 RELATED WORK

**EEG Decoding and Generalization** EEG decoding has evolved from handcrafted features to deep architectures, with EEGNet emerging as a widely adopted baseline due to its efficient depthwise–separable convolutions and lightweight design (Lawhern et al., 2018). Recent models explore transformers (Liao et al., 2025; Song et al., 2022a) and graph neural networks (Tang et al., 2024; Hu et al., 2023), but EEGNet remains favored for its robustness and simplicity. A key limitation is poor cross-subject generalization, with 20–40% accuracy drops despite strong within-subject perfor-

054  
055  
056  
057  
058  
059  
060  
061  
062  
063  
064  
065  
066  
067  
068  
069  
070  
071  
072  
073  
074  
075  
076  
077  
078  
079  
080  
081  
082  
083  
084  
085  
086  
087  
088  
089  
090  
091  
092  
093  
094  
095  
096  
097  
098  
099  
100  
101  
102  
103  
104  
105  
106  
107  
mance (Huang et al., 2023; Barmpas et al., 2023). Attempts to address this require expensive calibration (Rommel et al., 2022; Liu et al., 2022; Wu, 2016). Scalable BCIs require subject-agnostic models that generalize without per-user retraining.

**Diffusion Models for EEG** Denoising Diffusion Probabilistic Models (DDPMs) model data distributions via iterative denoising and outperform GANs in EEG synthesis by avoiding mode collapse (Tosato et al., 2023; Ho et al., 2020). Recent enhancements, such as reinforcement learning (An et al., 2024) and progressive distillation (Torma & Szegletes, 2025), have further improved realism and sampling speed. Diff-E (Kim et al., 2023) extended diffusion to imagined-speech decoding via joint reconstruction and classification, but remained task-specific and did not address cross-subject generalization. Broader research suggests that combining generative and discriminative objectives yields stronger representations (Chow et al., 2024; Grathwohl et al., 2019), yet EEG models typically optimize only one. We explore this joint learning paradigm across diverse EEG tasks, aiming to learn generalizable representations that capture both signal structure and task-relevant information.

**Mixup Methods** Signal-level augmentation has evolved from basic jittering and filtering to temporal, spectral, and channel-wise mixup (Luo & Cai, 2025; Liu et al., 2025; Kim et al., 2021; Pei et al., 2021; Zhang et al., 2017), but many variants introduce unrealistic artifacts that hinder generalization. This motivates our systematic evaluation of weighted and temporal input mixup across encoder layers, along with latent-space mixing

**Evaluation Strategies** Effective cross-subject EEG decoding requires both rigorous training strategies and standardized evaluation. Leave-one-subject-out (LOSO) validation remains common but is computationally intensive and impractical for real-time deployment (Del Pup et al., 2025; Chen et al., 2025; Zhao et al., 2024; Barmpas et al., 2023; Kunjan et al., 2021), while simpler subject splits often neglect session independence and true seen/unseen separation (Zhang et al., 2023). We address it in our work by introducing a standardized subject- and session-disjoint evaluation.

### 3 METHODOLOGY

#### 3.1 MULTIDIFFNET ARCHITECTURE

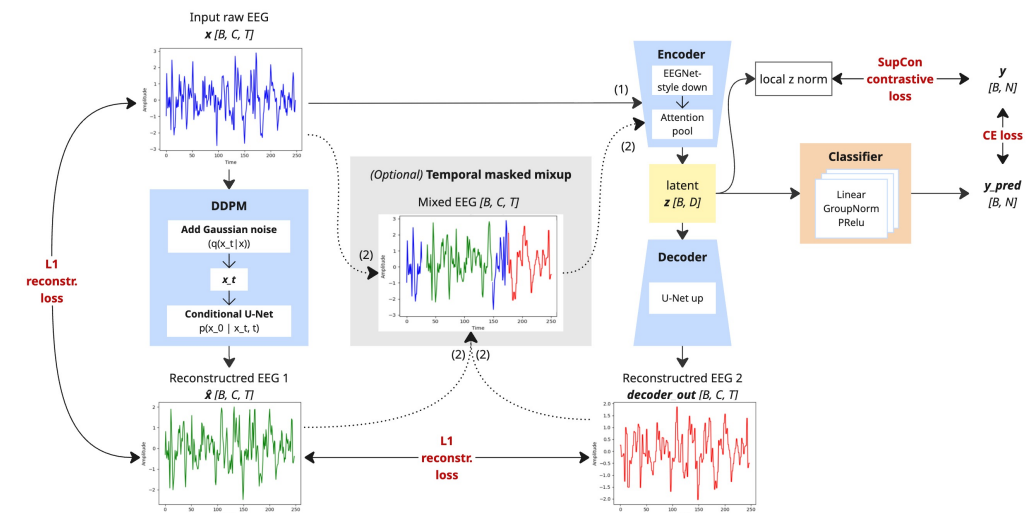


Figure 1: Overview of the *MultiDiffNet* that jointly optimizes a conditional DDPM, a contrastive encoder, and a generative decoder through a shared latent space  $z$ . The encoder produces discriminative features used for both classification and contrastive learning, while the decoder and DDPM reconstruct the input signal. An optional *temporal masked mixup* module stochastically blends the original, DDPM-denoised, and decoder-reconstructed EEG to improve representation quality.

---

108 *MultiDiffNet* is a modular architecture designed to jointly optimize classification, reconstruction, and  
109 contrastive structure learning from EEG signals. It consists of a Denoising Diffusion Probabilistic  
110 Model (DDPM), a discriminative encoder, a generative decoder, and a classifier (Figure 1).

111 Given a raw EEG signal  $x \in \mathbb{R}^{C \times T}$ , where  $C$  is the number of EEG channels and  $T$  is the number of  
112 timepoints, the model processes the input in two parallel paths. First, the DDPM denoises the signal  
113 via a learned reverse diffusion process, producing a refined version  $\hat{x} \in \mathbb{R}^{C \times T}$ . Simultaneously,  
114 the same input  $x$  is passed through an EEGNet-based encoder (See Section 3.2) to extract a latent  
115 representation  $z \in \mathbb{R}^D$ , where  $D$  is the embedding dimension. The latent vector  $z$  is then used for  
116 two purposes: (1) it is passed to a lightweight decoder to reconstruct the denoised signal  $\hat{x}$ , resulting  
117 in a reconstruction  $x_{\text{dec}} \in \mathbb{R}^{C \times T}$ ; and (2) it is passed to a fully connected classification head to  
118 predict class logits  $\hat{y} \in \mathbb{R}^K$ , where  $K$  is the number of classes.

119 To further structure the latent space,  $z$  is locally normalized (Section 3.3) and then projected to  
120  $z_{\text{proj}} \in \mathbb{R}^{D'}$ , which is optimized with a supervised contrastive loss. All classification and reconstruc-  
121 tion are performed directly from  $z$ , without relying on generated augmentations.

122 We performed an extensive ablation study across architectural variants, modifying the presence of  
123 DDPMs, encoder inputs, decoder pathways, classifier heads, and loss terms. The configuration de-  
124 scribed here reflects the best-performing combination.

### 126 3.2 EEGNET-STYLE ENCODER WITH ATTENTION POOL

128 Given EEGNet’s demonstrated effectiveness across multiple EEG decoding tasks, we adapt its ar-  
129 chitecture as our discriminative encoder, hypothesizing that its proven feature extraction capabilities  
130 can produce powerful latent representations  $z$  for our multi-objective framework. Our encoder ex-  
131 tracts multi-scale features ( $dn_1, dn_2, dn_3$ ) from different layers and applies attention pooling:

132 
$$z = \text{AttentionPool}(dn_3) \in \mathbb{R}^D,$$

### 135 3.3 SUBJECT-WISE LATENT NORMALIZATION

136 To mitigate inter-subject variability, we apply subject-wise normalization on the encoder output  $z$ :

138 
$$z_{\text{norm}} = \frac{z - \mu_s}{\sigma_s},$$

140 where  $\mu_s$  and  $\sigma_s$  denote the mean and standard deviation computed per subject  $s$  using a subset of  
141 training trials. During evaluation, we adopt a two-mode strategy: for seen subjects, normalization  
142 uses pre-computed statistics from their training data; for unseen subjects, statistics are estimated  
143 on-the-fly using their own calibration trials, simulating realistic deployment scenarios.

### 145 3.4 MIXUP STRATEGIES

147 Mixup strategies can improve robustness in low-trial EEG decoding. However, standard mixup tech-  
148 niques may not fully exploit the structure of neural time series. We therefore explore two comple-  
149 mentary strategies: *Weighted Average Mixup* and a novel *Temporal Masked Mixup*. *Weighted Average*  
150 *Mixup* performs linear interpolation between the original EEG input  $x$ , the DDPM-denoised out-  
151 put  $\hat{x}$ , and the decoder reconstruction  $x_{\text{dec}}$ . We investigate multiple integration points in the model:  
152 **(0)** Input-level mixup, **(1-3)** Mixup after encoder layers 1, 2, or 3, respectively, **(4)** Mixup after the  
153 final attention pooling layer. To address the limitations of global interpolation, we propose *Temporal*  
154 *Masked Mixup*, which perturbs only localized segments of the input time series while preserving  
155 surrounding structure. See Algorithm 1 for pseudocode.

### 156 3.5 LOSS FUNCTIONS

158 *MultiDiffNet* is trained using a weighted sum of three objectives:

159 
$$\mathcal{L}_{\text{total}} = \underbrace{\alpha \mathcal{L}_{\text{CE/MSE}}(\hat{y}, y)}_{\text{classification}} + \underbrace{\beta \mathcal{L}_{\text{L1}}(x_{\text{dec}}, \hat{x})}_{\text{reconstruction}} + \underbrace{\gamma \mathcal{L}_{\text{SupCon}}(z_{\text{proj}}, y)}_{\text{contrastive}}$$

---

162 **Algorithm 1** Temporal Masked Mixup

---

163 1: Initialize a binary mask  $M \in \{0, 1\}^{C \times T}$  with all zeros.  
164 2: Flip each 0 in  $M$  to 1 with probability  $p = 0.01$ .  
165 3: **for** each position in  $M$  with value 1 **do**  
166 4:     Expand to a temporal window of random length (uniform between min and max size).  
167 5: **end for**  
168 6: Flip each 1 in  $M$  to  $-1$  with:  
169     • Fixed probability 0.5 (**fixed ratio**), or  
170     • Probability drawn from Beta(0.2, 0.2) each epoch (**random ratio**).  
171 7: Apply the final mask:  
172     •  $0 \rightarrow x$  (original input)  
173     •  $1 \rightarrow \hat{x}$  (DDPM output)  
174     •  $-1 \rightarrow x_{\text{dec}}$  (decoder output)

---

175

176 We fix  $\alpha = 1.0$  and progressively scale  $\beta$  and  $\gamma$  to stabilize training:

177

$$\beta = \min \left( 1.0, \frac{\text{epoch}}{100} \right) \cdot 0.05, \quad \gamma = \min \left( 1.0, \frac{\text{epoch}}{50} \right) \cdot 0.2$$

178 Details on loss formulation and weighting strategies are provided in the Appendix.

179 3.6 EVALUATION METRICS

180 We evaluate model performance primarily using downstream classification accuracy, which quantifies the proportion of correctly classified EEG samples. Accuracy is defined as:

181

$$\text{Accuracy} = \frac{TP + TN}{TP + TN + FP + FN}$$

182 where  $TP$ ,  $TN$ ,  $FP$ , and  $FN$  denote true positives, true negatives, false positives, and false negatives, respectively. In addition, we report F1 score, precision, recall, and AUC for a more comprehensive evaluation; detailed formulas and results are provided in the Appendix.

183 3.7 TREND-LEVEL STATISTICAL REPORTING FRAMEWORK

184 Conventional  $p$ -values often fail under the high-variance, low-trial, subject-disjoint conditions of EEG decoding. To address this, we introduce a robust trend-level statistical framework (detailed in the Appendix) that synthesizes effect sizes, cross-seed consistency, and Bayesian posterior probabilities. This allows us to detect systematic, reproducible gains even when classical significance tests return null results. Our approach represents a principled shift toward reproducible, evidence-based model evaluation in brain decoding.

185 While this framework enhances reproducibility, it is not meant to substitute conventional  $p$ -value testing. Instead, it addresses a well-documented limitation: in low-trial, high-variance EEG decoding, even systematic improvements may fail to reach arbitrary significance thresholds. Such small yet consistent gains—for instance, 2–3% accuracy in imagined speech or SSVEP—can substantially affect usability in BCI systems. By combining effect sizes, cross-seed consistency, and Bayesian evidence, the framework provides a principled way to surface these domain-relevant improvements, while remaining fully compatible with classical and non-parametric statistical tests.

186 4 EXPERIMENTS AND RESULTS

187 4.1 BENCHMARK DATASET SUITE

188 We curated four diverse EEG benchmarks (SSVEP, P300, Motor Imagery, and Imagined Speech), spanning increasing decoding difficulty. Each dataset is split into train, val, and two test sets: a seen-subject (intra-subject) split and an unseen-subject (cross-subject) split. This standardized protocol

216

217

218

219

220

221

222

223

224

225

226

227

228

229

Figure 2: Overview of four EEG datasets ranked by task difficulty from easiest (top) to hardest (bottom). Task paradigms and preprocessing details are adapted from the original publications: SSVEP Wang et al. (2017), P300 Korczowski et al. (2019), Motor Imagery Tangermann et al. (2012), and Imagined Speech Zhao & Rudzicz (2015).

234

235

enables rigorous evaluation of both personalization and generalization, addressing the inconsistent and often unrealistic split practices prevalent in prior EEG research, where models are evaluated on mixed subject data or using computationally expensive LOSO.

239

240

## 4.2 BASELINES

241

242

243

244

We benchmarked our model against a diverse set of carefully selected baselines to ensure robust and fair comparisons. Our selection criteria were twofold: (i) prioritize architectures that are widely used for generalization to unseen subjects or sessions, and (ii) cover the main inductive biases found in EEG decoding, such as spatial filtering, temporal modeling, and attention mechanisms.

245

246

247

248

249

250

251

252

253

254

Specifically, we include: (1) **EEGNet** (Lawhern et al., 2018), a compact depthwise-separable CNN that is widely adopted for cross-subject generalization due to its strong accuracy–efficiency trade-off; (2) **ShallowFBCSPNet** (Schirrmeister et al., 2017), which implements learnable filter-bank Common Spatial Patterns (CSP) to extract frequency–spatial features; (3) **TIDNet** (Kostas & Rudzicz, 2020), which introduces dilated convolutions and residual connections to improve robustness under subject shift; (4) **EEGConformer** (Song et al., 2022b), which combines a convolutional front-end with self-attention to model both local spatial structure and global temporal context; and (5) **EEGTCNet** (Ingolfsson et al., 2020), a temporal convolutional network tailored for EEG that emphasizes causal and dilated temporal modeling, offering complementary inductive bias to purely spatial–spectral models.

255

256

257

258

All models are evaluated using identical input windows of shape  $(C, T)$ , and trained with a unified global training schedule to ensure comparability. Public implementations and recommended hyperparameters are used where available, with no method-specific tuning.

259

260

## 4.3 GENERALIZATION PERFORMANCE

261

262

263

264

265

266

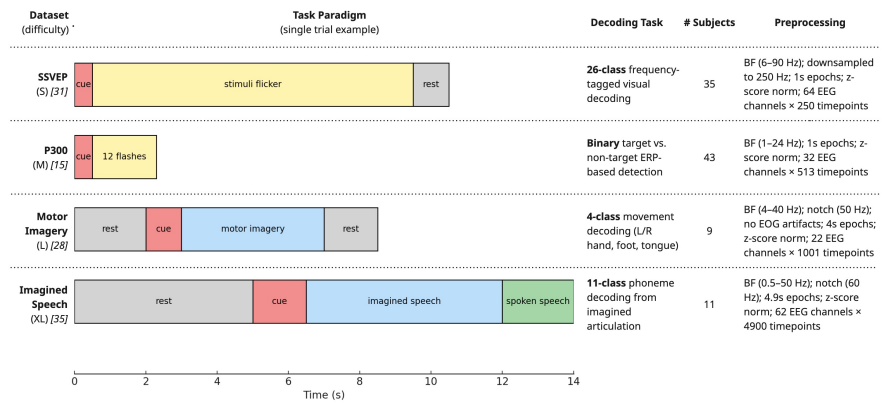
267

268

269

*MultiDiffNet* helps with generalization. Unlike raw EEG representations, where class boundaries blur due to subject-specific noise, our learned latent space forms clearly separable, label-aligned clusters (Figure 3). This structured representation enables robust decoding across subjects. As shown in Table 1, *MultiDiffNet* consistently reduces the seen–unseen accuracy gap across all tasks. In SSVEP, it lifts cross-subject accuracy from 81.08% (EEGNet baseline) to 84.72%, further boosted to 85.25% with Temporal Masked Mixup. For comparison, other representative architectures such as ShallowFBCSPNet (58.87%), EEGConformer (51.92%), TIDNet (25.96%), and EEGTCNet (49.57%) fall well behind, highlighting the robustness of our latent-space design.

Even in the low-SNR regime of Imagined Speech, *MultiDiffNet* improves cross-subject accuracy from 10.61% (EEGNet) to 12.12%, while simultaneously achieving a much larger gain on seen-



270  
 271 Table 1: Final results across tasks and models. Accuracy is reported for both seen-subject (intra-  
 272 subject) and unseen-subject (cross-subject) test splits. Tasks are ranked by task difficulty. *Stars de-*  
 273 *note win percentage: \*\*\* ≥ 80%, \*\* ≥ 60%, \* ≥ 40%. Detailed results are in the Appendix.*

276	Task	Model	Subj.	Classes	Seen Acc. (%)	Unseen (%)	Acc.
277	SSVEP	ShallowFBCSPNet	35	26	69.58 ± 1.30*	58.87 ± 9.37*	
278		EEGConformer	35	26	66.98 ± 2.83	51.92 ± 9.06	
279		TIDNet	35	26	28.01 ± 4.12	25.96 ± 5.29	
280		EEGTCNet	35	26	58.31 ± 4.02	49.57 ± 9.14	
281		EEGNet	35	26	89.16 ± 0.57***	81.08 ± 9.16**	
282		<b>MultiDiffNet</b>	35	26	85.08 ± 1.53**	<b>84.72 ± 6.03***</b>	
283		<b>MultiDiffNet + Mixup</b>	35	26	86.79 ± 1.75***	<b>85.25 ± 6.94***</b>	
284	P300	ShallowFBCSPNet	43	2	87.72 ± 0.33	86.20 ± 1.45	
285		EEGConformer	43	2	88.54 ± 0.54**	86.30 ± 1.73	
286		TIDNet	43	2	88.24 ± 0.31*	85.63 ± 0.58**	
287		EEGTCNet	43	2	88.69 ± 0.59***	87.02 ± 1.62***	
288		EEGNet	43	2	88.79 ± 0.67***	87.24 ± 2.01***	
289		<b>MultiDiffNet</b>	43	2	85.35 ± 1.12	79.47 ± 0.54*	
290		<b>MultiDiffNet + Mixup</b>	43	2	85.61 ± 0.52	79.56 ± 4.43	
291	MI	ShallowFBCSPNet	9	4	64.34 ± 3.61***	36.46 ± 6.60	
292		EEGConformer	9	4	59.57 ± 5.60**	36.49 ± 7.72	
293		TIDNet	9	4	44.27 ± 2.60	34.42 ± 3.60	
294		EEGTCNet	9	4	58.85 ± 4.54	32.99 ± 6.94	
295		EEGNet	9	4	67.01 ± 5.38***	46.18 ± 7.20***	
296		<b>MultiDiffNet</b>	9	4	55.85 ± 2.80	39.24 ± 8.00***	
297		<b>MultiDiffNet + Mixup</b>	9	4	57.69 ± 3.27*	36.78 ± 5.23	
298	Img. Speech	ShallowFBCSPNet	11	11	13.78 ± 1.55**	10.48 ± 0.64	
299		EEGConformer	11	11	10.62 ± 0.82	9.21 ± 3.00	
300		TIDNet	11	11	9.10 ± 0.54	10.35 ± 0.18	
301		EEGTCNet	11	11	12.64 ± 1.58	10.10 ± 0.64	
302		EEGNet	11	11	11.26 ± 2.01*	10.61 ± 0.93*	
303		<b>MultiDiffNet</b>	11	11	<b>15.55 ± 0.62***</b>	<b>11.62 ± 1.29***</b>	
304		<b>MultiDiffNet + Mixup</b>	11	11	<b>17.57 ± 1.16***</b>	<b>12.12 ± 0.38***</b>	

306 subject accuracy (11.26% → 17.57%). Other baselines such as ShallowFBCSPNet (10.48/13.78%),  
 307 EEGConformer (9.21/10.62%), TIDNet (10.35/9.10%), and EEGTCNet (10.10/12.64%) hover close  
 308 to chance level on both splits, further highlighting the robustness of our approach. For such a chal-  
 309 lengeing task, even modest absolute gains are meaningful, as they can indicate more reliable signal ex-  
 310 traction under extreme noise conditions. On Motor Imagery, *MultiDiffNet* also surpasses most base-  
 311 lines on unseen accuracy, e.g., outperforming TIDNet (34.42%) and EEGTCNet (32.99%), while  
 312 maintaining competitive seen accuracy (57.69% vs. 44.27% for TIDNet and 58.85% for EEGTC-  
 313 Net). Although it remains slightly below EEGNet (46.18/67.01%), this is likely due to ceiling effects  
 314 and dataset scale.

#### 315 4.4 ABLATION STUDIES

316 To understand what drives generalization in *MultiDiffNet*, we ran extensive ablation experiments,  
 317 over 100 controlled configs. All results are reported for both seen- and unseen-subject accuracy,  
 318 with statistical evidence matrices and trend-level effect sizes in the Appendix.

319 **Decoder input.** Feeding only  $z$  to the decoder often matches or exceeds more complex fusion vari-  
 320 ants. For example, SSVEP unseen accuracy reaches 84.72% with  $z$  alone, further boosted to 85.25%  
 321 with mixup, while more elaborate fusions ( $z + x$ ,  $x_{\text{hat}} + \text{skips}$ ) show no consistent gains. These  
 322 findings validate our architectural decision to decode primarily from  $z$ . For completeness, the best

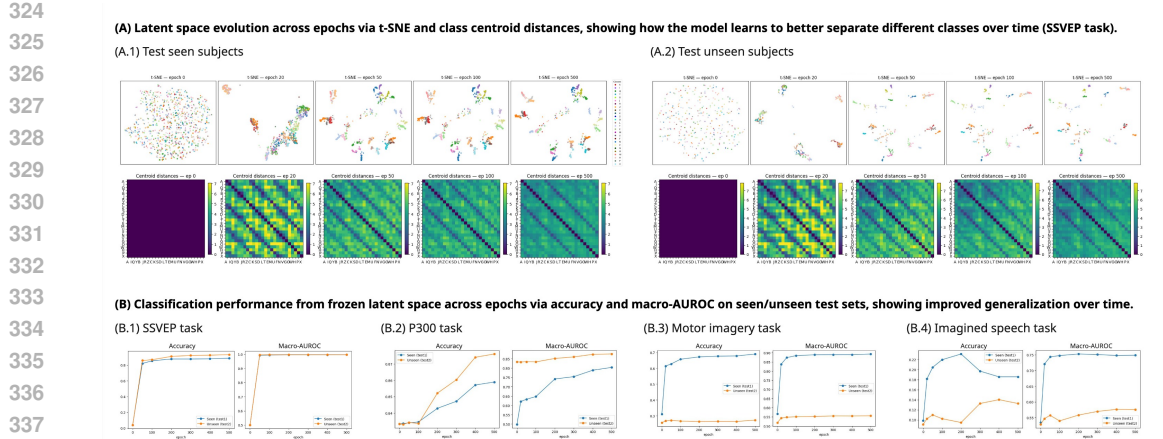


Figure 3: (A) Visualization of latent space across training epochs. (B) Downstream classification performance from frozen latent representations.

accuracies achieved in this ablation are 85.86/84.72 on SSVEP, 85.88/81.41 on P300, 56.89/40.36 on Motor Imagery, and 18.58/12.88 on Imagined Speech (seen/unseen).

**Classifier head.** A lightweight FC head on  $z$  delivers state-of-the-art generalization with minimal complexity. It rivals or outperforms EEGNet classifiers trained on  $x$ , especially in low-SNR tasks. This supports our choice to use FC as the default classification head. For completeness, the best accuracies achieved in this ablation are 85.08/84.72 on SSVEP, 85.35/84.12 on P300, 55.85/39.24 on Motor Imagery, and 17.95/11.61 on Imagined Speech (seen/unseen).

**Encoder and decoder.** Using raw  $x$  as encoder input consistently outperforms  $\hat{x}$ , showing that denoising is useful for regularization. Interestingly, removing the decoder entirely sometimes improves generalization, suggesting that reconstruction may introduce noise if overemphasized. For completeness, the best accuracies in this ablation are 90.95/85.58 on SSVEP, 85.71/80.93 on P300, 55.85/40.16 on Motor Imagery, and 19.22/13.76 on Imagined Speech (seen/unseen).

**Loss combinations.** Combining CE with mild MSE or contrastive losses improves stability, particularly when auxiliary weights are gently annealed. The best results use  $\beta = 0.05, \gamma = 0.2$ —balancing reconstruction as a regularizer without overpowering the classification objective. For completeness, the best accuracies in this ablation are 86.40/85.58 on SSVEP, 85.69/80.18 on P300, 59.67/41.44 on Motor Imagery, and 19.60/13.51 on Imagined Speech (seen/unseen).

**Mixup strategies.** Mixup effects are task-specific. For SSVEP, *Temporal Masked Mixup* outperforms all variants. Motor Imagery benefits from *Weighted Average Mixup*, while P300 and Imagined Speech show limited sensitivity, highlighting that mixup is most impactful in high-SNR regimes. For completeness, the best accuracies in this ablation are 87.84/85.26 on SSVEP, 85.78/79.56 on P300, 63.44/38.83 on Motor Imagery, and 19.47/12.12 on Imagined Speech (seen/unseen).

## 5 CONCLUSIONS AND FUTURE WORK

We presented *MultiDiffNet*, a diffusion-based neural decoder that learns a compact, multi-objective latent space for EEG decoding without synthetic augmentation. Through unified benchmarks and rigorous cross-subject evaluation, we showed that *MultiDiffNet* achieves strong generalization across diverse BCI paradigms, particularly in challenging low-signal settings such as SSVEP and Imagined Speech. Our statistical analysis framework further addresses reproducibility challenges in low-trial EEG research. Future work will explore scaling *MultiDiffNet* to larger and more diverse EEG datasets and extending the architecture to other neural modalities.

For completeness, we note that our trend-level statistical framework is intended only as a complementary tool for low-trial EEG research; detailed rationale is provided in Section 3.7, with Bayesian and non-parametric validations reported in the Appendix.

---

378      REFERENCES  
379

380      Hossein Ahmadi and Luca Mesin. Universal semantic feature extraction from eeg signals: a task-  
381      independent framework. *Journal of Neural Engineering*, 22(3):036003, 2025.

382      Yang An, Yuhao Tong, Weikai Wang, and Steven W. Su. Enhancing eeg signal generation through  
383      a hybrid approach integrating reinforcement learning and diffusion models, 2024. URL <https://arxiv.org/abs/2410.00013>.

384

385      Konstantinos Barmpas, Yannis Panagakis, Stylianos Bakas, Dimitrios A Adamos, Nikolaos  
386      Laskaris, and Stefanos Zafeiriou. Improving generalization of cnn-based motor-imagery eeg  
387      decoders via dynamic convolutions. *IEEE Transactions on Neural Systems and Rehabilitation  
388      Engineering*, 31:1997–2005, 2023.

389

390      Ziheng Chen, Po T Wang, Mina Ibrahim, Shivali Baveja, Rong Mu, An H Do, and Zoran Nenadic.  
391      Leveraging transfer learning and user-specific updates for rapid training of bci decoders. *arXiv  
392      preprint arXiv:2506.14120*, 2025.

393

394      Wei Chow, Juncheng Li, Qifan Yu, Kaihang Pan, Hao Fei, Zhiqi Ge, Shuai Yang, Siliang Tang,  
395      Hanwang Zhang, and Qianru Sun. Unified generative and discriminative training for multi-modal  
396      large language models. *Advances in Neural Information Processing Systems*, 37:23155–23190,  
397      2024.

398

399      Federico Del Pup, Andrea Zanola, Louis Fabrice Tshimanga, Alessandra Bertoldo, Livio Finos, and  
400      Manfredo Atzori. The role of data partitioning on the performance of eeg-based deep learning  
401      models in supervised cross-subject analysis: a preliminary study. *Computers in Biology and  
Medicine*, 196:110608, 2025.

402

403      Will Grathwohl, Kuan-Chieh Wang, Jörn-Henrik Jacobsen, David Duvenaud, Mohammad Norouzi,  
404      and Kevin Swersky. Your classifier is secretly an energy based model and you should treat it like  
405      one. *arXiv preprint arXiv:1912.03263*, 2019.

406

407      He Gu, Tingwei Chen, Xiao Ma, Mengyuan Zhang, Yan Sun, and Jian Zhao. Cltnet: A hybrid deep  
408      learning model for motor imagery classification. *Brain Sciences*, 15(2):124, 2025.

409

410      Kay Gregor Hartmann, Robin Tibor Schirrmacher, and Tonio Ball. Eeg-gan: Generative adversarial  
411      networks for electroencephalographic (eeg) brain signals. *arXiv preprint arXiv:1806.01875*, 2018.

412

413      Jonathan Ho, Ajay Jain, and Pieter Abbeel. Denoising diffusion probabilistic models. *Advances in  
414      neural information processing systems*, 33:6840–6851, 2020.

415

416      Wanyu Hu, Guoqian Jiang, Junxia Han, Xiaoli Li, and Ping Xie. Regional-asymmetric adaptive  
417      graph convolutional neural network for diagnosis of autism in children with resting-state eeg.  
418      *IEEE Transactions on Neural Systems and Rehabilitation Engineering*, 32:200–211, 2023.

419

420      Gan Huang, Zhiheng Zhao, Shaorong Zhang, Zhenxing Hu, Jiaming Fan, Meisong Fu, Jiale Chen,  
421      Yaqiong Xiao, Jun Wang, and Guo Dan. Discrepancy between inter-and intra-subject variability  
422      in eeg-based motor imagery brain-computer interface: Evidence from multiple perspectives.  
423      *Frontiers in neuroscience*, 17:1122661, 2023.

424

425      T. M. Ingolfsson, M. Hersche, X. Wang, N. Kobayashi, L. Cavigelli, and L. Benini. Eeg-tcnet:  
426      An accurate temporal convolutional network for embedded motor-imagery brain–machine interfaces.  
427      *arXiv preprint arXiv:2006.00622*, 2020. URL <https://doi.org/10.48550/arXiv.2006.00622>.  
428      EEGTCNet.

429

430      Gwantae Kim, David K Han, and Hanseok Ko. Specmix: A mixed sample data augmentation method  
431      for training withtime-frequency domain features. *arXiv preprint arXiv:2108.03020*, 2021.

432

433      Soowon Kim, Young-Eun Lee, Seo-Hyun Lee, and Seong-Whan Lee. Diff-e: Diffusion-based learn-  
434      ing for decoding imagined speech eeg. *arXiv preprint arXiv:2307.14389*, 2023.

435

436      Louis Korczowski, Martine Cederhout, Anton Andreev, Grégoire Cattan, Pedro Luiz Coelho Ro-  
437      drigues, Violette Gautheret, and Marco Congedo. *Brain Invaders calibration-less P300-based  
438      BCI with modulation of flash duration Dataset (bi2015a)*. PhD thesis, GIPSA-lab, 2019.

---

432 Dimitrios Kostas and Frank Rudzicz. Thinker invariance: Enabling deep neural networks for  
433 bci across more people. *Journal of Neural Engineering*, 17(5):056008, 2020. doi: 10.1088/  
434 1741-2552/abb7a7. TIDNet.

435

436 Sajeet Kunjan, Tyler S Grummert, Kenneth J Pope, David MW Powers, Sean P Fitzgibbon, T Bas-  
437 tiampillai, M Battersby, and Trent W Lewis. The necessity of leave one subject out (losos) cross  
438 validation for eeg disease diagnosis. In *International conference on brain informatics*, pp. 558–  
439 567. Springer, 2021.

440 Vernon J Lawhern, Amelia J Solon, Nicholas R Waytowich, Stephen M Gordon, Chou P Hung, and  
441 Brent J Lance. Eegnet: a compact convolutional neural network for eeg-based brain–computer  
442 interfaces. *Journal of neural engineering*, 15(5):056013, 2018.

443

444 Young-Eun Lee and Seo-Hyun Lee. Eeg-transformer: Self-attention from transformer architecture  
445 for decoding eeg of imagined speech. In *2022 10th International winter conference on brain-  
446 computer interface (BCI)*, pp. 1–4. IEEE, 2022.

447

448 Wangdan Liao, Hongyun Liu, and Weidong Wang. Advancing bci with a transformer-based model  
449 for motor imagery classification. *Scientific Reports*, 15(1):23380, 2025.

450

451 Siwei Liu, Jia Zhang, Andong Wang, Hanrui Wu, Qibin Zhao, and Jinyi Long. Subject adapta-  
452 tion convolutional neural network for eeg-based motor imagery classification. *Journal of Neural  
453 Engineering*, 19(6):066003, 2022.

454

455 Xuan-Hao Liu, Bao-Liang Lu, and Wei-Long Zheng. mixeeg: Enhancing eeg federated learning for  
456 cross-subject eeg classification with tailored mixup. *arXiv preprint arXiv:2504.07987*, 2025.

457

458 Tian-jian Luo and Zikun Cai. Diffusion models-based motor imagery eeg sample augmentation via  
459 mixup strategy. *Expert Systems with Applications*, 235:125585, 2024. doi: 10.1016/j.eswa.2024.  
460 125585. URL <https://www.sciencedirect.com/science/article/pii/S0957417424024527>.

461

462 Tian-jian Luo and Zikun Cai. Diffusion models-based motor imagery eeg sample augmentation via  
463 mixup strategy. *Expert Systems with Applications*, 262:125585, 2025.

464

465 Yu Pei, Zhiguo Luo, Ye Yan, Huijong Yan, Jing Jiang, Weiguo Li, Liang Xie, and Erwei Yin.  
466 Data augmentation: Using channel-level recombination to improve classification performance for  
467 motor imagery eeg. *Frontiers in Human Neuroscience*, 15:645952, 2021.

468

469 Cédric Rommel, Joseph Paillard, Thomas Moreau, and Alexandre Gramfort. Data augmentation for  
470 learning predictive models on eeg: a systematic comparison. *Journal of Neural Engineering*, 19  
471 (6):066020, 2022.

472

473 Robin T Schirrmeister, Jost T Springenberg, Lorenz DJ Fiederer, Markus Glasstetter, Katharina  
474 Eggensperger, Michael Tangermann, Frank Hutter, and Tonio Ball. Deep learning with convolu-  
475 tional neural networks for eeg decoding and visualization. *Human Brain Mapping*, 2017. doi:  
476 10.1002/hbm.23730. URL <http://dx.doi.org/10.1002/hbm.23730>. ShallowFBCSPNet.

477

478 Yonghao Song, Qingqing Zheng, Bingchuan Liu, and Xiaorong Gao. Eeg conformer: Convolu-  
479 tional transformer for eeg decoding and visualization. *IEEE Transactions on Neural Systems and  
480 Rehabilitation Engineering*, 31:710–719, 2022a.

481

482 Yujie Song, Qinglin Zheng, Bo Liu, and Xiaorong Gao. Eeg conformer: Convolutional transformer  
483 for eeg decoding and visualization. *IEEE Transactions on Neural Systems and Rehabilitation  
484 Engineering*, 31:710–719, 2022b. doi: 10.1109/TNSRE.2022.3223706. URL <https://ieeexplore.ieee.org/document/9991178>. EEGConformer.

485

486 Xianlun Tang, Jing Zhang, Yidan Qi, Ke Liu, Rui Li, and Huiming Wang. A spatial filter tempo-  
487 ral graph convolutional network for decoding motor imagery eeg signals. *Expert Systems with  
488 Applications*, 238:121915, 2024.

489

490 Michael Tangermann, Klaus-Robert Müller, Ad Aertsen, Niels Birbaumer, Christoph Braun,  
491 Clemens Brunner, Robert Leeb, Carsten Mehring, Kai J Miller, Gernot R Müller-Putz, et al. Re-  
492 view of the bci competition iv. *Frontiers in neuroscience*, 6:55, 2012.

---

486 Szabolcs Torma and Luca Szegletes. Generative modeling and augmentation of eeg signals using  
487 improved diffusion probabilistic models. *Journal of Neural Engineering*, 22(1):016001, 2025.  
488 doi: 10.1088/1741-2552/ada0e4.

489 Giulio Tosato, Cesare M. Dalbagno, and Francesco Fumagalli. Eeg synthetic data generation using  
490 probabilistic diffusion models, 2023. URL <https://arxiv.org/abs/2303.06068>.

492 Yijun Wang, Xiaogang Chen, Xiaorong Gao, and Shangkai Gao. A benchmark dataset for ssvep-  
493 based brain-computer interfaces. *IEEE Transactions on Neural Systems and Rehabilitation Engi-*  
494 *neering*, 25(10):1746–1752, 2017. doi: 10.1109/TNSRE.2016.2578980. URL <https://ieeexplore.ieee.org/document/7740878>.

496 Dongrui Wu. Online and offline domain adaptation for reducing bci calibration effort. *IEEE Trans-*  
497 *actions on human-machine Systems*, 47(4):550–563, 2016.

499 Hao Zhang, Hongfei Ji, Jian Yu, Jie Li, Lingjing Jin, Lingyu Liu, Zhongfei Bai, and Chen Ye.  
500 Subject-independent eeg classification based on a hybrid neural network. *Frontiers in Neuro-*  
501 *science*, 17:1124089, 2023.

502 Hongyi Zhang, Moustapha Cisse, Yann N Dauphin, and David Lopez-Paz. mixup: Beyond empirical  
503 risk minimization. *arXiv preprint arXiv:1710.09412*, 2017.

505 Shunan Zhao and Frank Rudzicz. Classifying phonological categories in imagined and articu-  
506 lated speech. In *2015 IEEE international conference on acoustics, speech and signal processing*  
507 (*ICASSP*), pp. 992–996. IEEE, 2015.

508 Wei Zhao, Xiaolu Jiang, Baocan Zhang, Shixiao Xiao, and Sujun Weng. Ctnet: a convolutional  
509 transformer network for eeg-based motor imagery classification. *Scientific reports*, 14(1):20237,  
510 2024.

511  
512  
513  
514  
515  
516  
517  
518  
519  
520  
521  
522  
523  
524  
525  
526  
527  
528  
529  
530  
531  
532  
533  
534  
535  
536  
537  
538  
539